

## TWO-COMPONENT SECULAR GRAVITATIONAL INSTABILITY IN A PROTOPLANETARY DISK: A POSSIBLE MECHANISM FOR CREATING RING-LIKE STRUCTURES

SANEMICHI Z. TAKAHASHI<sup>1,2</sup>, SHU-ICHIRO INUTSUKA<sup>1</sup>

*Draft version March 27, 2018*

### ABSTRACT

The instability in protoplanetary disks due to gas-dust friction and self-gravity of gas and dust is investigated by linear analysis. In the case where the dust to gas ratio is enhanced and turbulence is weak, the instability grows, even in gravitationally stable disks, on a timescale of order  $10^{4-5}$ yr at a radius of order 100AU. If we ignore the dynamical feedback from dust grains in the gas equation of motion, the instability reduces to the so-called “secular gravitational instability”, which was investigated previously as an instability of dust in a fixed background gas flow. In this work, we solve the equations of motion for both gas and dust consistently and find that long-wavelength perturbations are stable, in contrast to the secular gravitational instability in the simplified treatment. This may indicate that we should not neglect small terms in equation of motion if the growth rate is small. The instability is expected to form ring structures in protoplanetary disks. The width of the ring formed at a radius of 100 AU is a few tens of AU. Therefore, the instability is a candidate for the formation mechanism of observed ring-like structures in disks. Another aspect of the instability is the accumulation of dust grains, and hence the instability may play an important role in the formation of planetesimals, rocky protoplanets, and cores of gas giants located at radii  $\sim 100$  AU. If these objects survive the dispersal of the gaseous component of the disk, they may be the origin of debris disks.

*Subject headings:* instabilities, protoplanetary disks

### 1. INTRODUCTION

Since planets are expected to form in protoplanetary disks, the formation and evolution of disks affect the planet formation process. In particular, terrestrial planets and cores of gas giants are expected to be formed via dust growth (Hayashi et al. 1985). Therefore, the dynamics of the dust in protoplanetary disks is essential to planet formation.

Recently, high-angular-resolution direct imaging of protoplanetary disks has become available. The observations reveal that ring structures are formed in protoplanetary disks (e.g. Fukagawa et al. 2006, 2013; Geers et al. 2007; Isella et al. 2010, 2012, 2013; Andrews et al. 2011; Hashimoto et al. 2011, 2012; Mathews et al. 2012; Mayama et al. 2012; Casassus et al. 2013; van der Marel et al. 2013). The formation mechanism of such structures remains unknown. One candidate for the formation mechanism is the density gap formed by gravitational interaction between the disk and unseen giant planets. (e.g. Lin & Papaloizou 1986, 1993; Takeuchi et al. 1996; Kley & Nelson 2012). However, planets have not been observed in most of the gaps. Moreover, Zhu et al. (2011) have mentioned that several planets are needed to make the observed wide gap. If planets are present in the gap, their maximum mass is estimated to be about five times the Jupiter mass (Hashimoto et al. 2011, 2012; Casassus et al. 2013). Since the sensitivity

of observations will increase, the maximum mass of the unseen planets will decrease and the observations will make clear whether rings are formed by planets.

In this work, we investigate a ring-formation mechanism without planets. We focus on instability due to gas-dust friction. This has been well studied, especially in the context of planetesimal formation. The streaming instability (Youdin & Goodman 2005; Youdin & Johansen 2007; Johansen & Youdin 2007) occurs via dust motion towards a central star (radial drift). The secular gravitational instability (secular GI, Ward 2000; Youdin 2011; Michikoshi et al. 2012) is the gravitational collapse of dust due to gas-dust friction. In a dust-rich disk the dust has large effect on the disk. Instability in dust rich disks has been investigated by Coradini et al. (1981). Recently, Lyra & Kuchner (2012, 2013) investigated the instability that occurs when gas is heated by dust via photoelectric heating in the debris disk, which contains more dust than gas.

In this work, we use full two-fluid equations for gas and dust in a typical gas-rich disk. We perform a local linear stability analysis and discuss whether the instability can explain the formation of the ring structures observed in protoplanetary disks. Although secular GI may also form dust rings, the analysis of secular GI only uses equations only for dust so secular GI cannot explain the observed ring structures of gas and dust (Mathews et al. 2012; Casassus et al. 2013; Fukagawa et al. 2013; van der Marel et al. 2013). Therefore, a linear analysis using equations for both gas and dust is needed to explain protoplanetary disk ring structures. We call the instability discussed in this paper “two-component secular GI”. In this work, we also take into account the effect of gas self-gravity.

This paper is organized as follows. The basic equations

<sup>1</sup>Department of Physics, Nagoya University, Furocho, Chikusa-ku, Nagoya, Aichi, 464-8602, Japan; takahashi.sanemichi@a.mbox.nagoya-u.ac.jp, inutsuka@nagoya-u.jp

<sup>2</sup>Department of Physics, Kyoto University, Oiwakecho, Kitashirakawa, Sakyo-ku, Kyoto 606-8502, Japan; sanemichi@tap.sphys.kyoto-u.ac.jp

for gas and dust for the linear analysis are given in Section 2. In Section 3 we derive the dispersion relation and parameter dependence of the maximum growth rate. We discuss the condition for the instability to grow in protoplanetary disks in Section 4. A summary is given in Section 5.

## 2. BASIC EQUATIONS

We investigate instability due to gas-dust friction in protoplanetary disks by using two fluid equations for both gas and dust. We focus on purely horizontal motions. We use the equations of continuity and motion for both gas and dust, and the Poisson equation:

$$\frac{\partial \Sigma}{\partial t} + \nabla \cdot (\Sigma \mathbf{u}) = 0, \quad (1)$$

$$\Sigma \left( \frac{\partial \mathbf{u}}{\partial t} + (\mathbf{u} \cdot \nabla) \mathbf{u} \right) = -c_s^2 \nabla \Sigma - \Sigma \nabla \left( \Phi - \frac{GM_*}{r} \right) + \frac{\Sigma_d (\mathbf{v} - \mathbf{u})}{t_{\text{stop}}}, \quad (2)$$

$$\frac{\partial \Sigma_d}{\partial t} + \nabla \cdot (\Sigma_d \mathbf{v}) = D \nabla^2 \Sigma, \quad (3)$$

$$\Sigma_d \left( \frac{\partial \mathbf{v}}{\partial t} + (\mathbf{v} \cdot \nabla) \mathbf{v} \right) = -\Sigma_d \nabla \left( \Phi - \frac{GM_*}{r} \right) + \frac{\Sigma_d (\mathbf{u} - \mathbf{v})}{t_{\text{stop}}}, \quad (4)$$

$$\nabla^2 \Phi = 4\pi G (\Sigma + \Sigma_d) \delta(z), \quad (5)$$

where  $\Sigma$  and  $\mathbf{u}$  are surface density and velocity of gas,  $\Sigma_d$  and  $\mathbf{v}$  are surface density and velocity of dust,  $c_s$  is the sound speed of gas,  $D$  is the diffusivity of the dust due to the gas turbulence,  $M_*$  is the central star mass, and  $t_{\text{stop}}$  is the stopping time of a dust particle.

We adopt a local shearing box model (e.g. Goldreich & Lynden-Bell 1965; Narayan et al. 1987). We focus on the neighborhood of a point  $(r, \theta) = (r_0, \Omega t)$  in cylindrical coordinates. The local radial and azimuthal coordinates are  $(x, y) = (r - r_0, r_0(\theta - \Omega t))$ . We adopt the Keplerian frequency,  $\Omega$ , at  $r = r_0$ ;  $\Omega = \sqrt{GM_*/r_0^3}$ . For simplicity, we assume axisymmetry.

We assume a steady state background with uniform surface density;  $\Sigma_0, \Sigma_{d0} = \text{const}$ ; dust-to-gas mass ratio  $\epsilon = \Sigma_{d0}/\Sigma_0$ ; and Keplerian rotation  $u_{x0} = v_{x0} = 0, u_{y0} = v_{y0} = (-3/2)\Omega_0 x$ . We decompose the physical quantities into background values and small perturbations proportional to  $\exp[ikx - i\omega t]$ . The linearized equations are given as follows:

$$-i\omega \delta \Sigma + ik \Sigma_0 \delta u_x = 0, \quad (6)$$

$$-i\omega \delta u_x - 2\Omega \delta u_y = -c_s^2 \frac{ik \delta \Sigma}{\Sigma_0} - ik \delta \Phi + \frac{\epsilon (\delta v_x - \delta u_x)}{t_{\text{stop}}}, \quad (7)$$

$$-i\omega \delta u_y + \frac{\Omega}{2} \delta u_x = \frac{\epsilon (\delta v_y - \delta u_y)}{t_{\text{stop}}}, \quad (8)$$

$$-i\omega \delta \Sigma_d + ik \epsilon \Sigma_0 \delta v_x = -D k^2 \delta \Sigma_d, \quad (9)$$

$$-i\omega \delta v_x - 2\Omega \delta v_y = -ik \delta \Phi + \frac{\delta u_x - \delta v_x}{t_{\text{stop}}}, \quad (10)$$

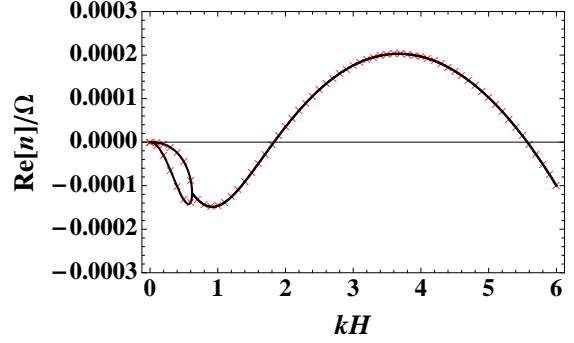


FIG. 1.— Dispersion relation of the unstable mode for  $t_{\text{stop}}\Omega = 0.01$ ,  $Q = 3$ ,  $\epsilon = 0.1$ ,  $D = 10^{-4}c_s^2\Omega^{-1}$ . The horizontal axis is the normalized wavenumber,  $kH$ , where  $H \equiv c_s/\Omega$  is the scale height of the gas disk. The vertical axis is the normalized growth rate of the instability,  $\text{Re}[n]/\Omega$ . The crosses show the exact solution given by Equations (6) to (12). The solid line shows the approximate solution given by Equation (13).

$$-i\omega \delta v_y + \frac{\Omega}{2} \delta v_x = \frac{\delta u_y - \delta v_y}{t_{\text{stop}}}, \quad (11)$$

$$\delta \Phi = -\frac{2\pi G (\delta \Sigma + \delta \Sigma_d)}{|k|}. \quad (12)$$

Hereafter we use the growth rate of the instability  $n \equiv -i\omega$  instead of the frequency  $\omega$ .

## 3. RESULTS

From the linearized equations derived in Section 2, we derive the dispersion relation for the instability. The dispersion relation given by Equations (6) to (12) is sixth order. Therefore, the dispersion relation implies six possible modes. Four modes are decaying oscillations with  $\text{Re}[n] < 0$  and  $\text{Im}[n] \neq 0$ . The other two modes can be unstable. Hereafter we investigate the unstable modes further.

### 3.1. Approximate Dispersion Relation

We provide approximate solutions of the dispersion relation and the condition for the instability. In the case  $n \ll t_{\text{stop}}^{-1}\Omega$  and  $t_{\text{stop}}\Omega \ll 1$  are satisfied, the dispersion relation is approximately given by the following quadratic equation,

$$\begin{aligned} & \left( \frac{1 + \epsilon}{t_{\text{stop}}} \right)^2 \left[ \Omega^2 - 2\pi G (1 + \epsilon) \Sigma_0 k + \frac{c_s^2 k^2}{1 + \epsilon} \right] n^2 \\ & + \left\{ \frac{\epsilon c_s^2 k^2}{t_{\text{stop}}} \left[ \Omega^2 - 2\pi G (1 + \epsilon) \Sigma k \right] \right. \\ & \left. + D k^2 \left( \frac{1 + \epsilon}{t_{\text{stop}}} \right)^2 \left[ \Omega^2 - 2\pi G \Sigma_0 k + \frac{c_s^2 k^2}{1 + \epsilon} \right] \right\} n \\ & + \frac{\epsilon c_s^2 k^2}{t_{\text{stop}}} \Omega^2 D k^2 = 0. \end{aligned} \quad (13)$$

Fig 1 shows the real part of the exact dispersion relation of the unstable modes for  $t_{\text{stop}}\Omega = 0.01$ ,  $\epsilon = 0.1$ ,  $D = 10^{-4}c_s^2\Omega^{-1}$ ,  $Q = 3$  and the real part of the approximate solution given by Equation (13), where  $Q \equiv c_s\Omega/\pi G\Sigma$  is Toomre's parameter. The figure indicates good agreement between the exact dispersion relation and the approximate one.

### 3.2. Conditions for Instability

There are two cases where the solutions of the Equation (13) have at least one positive real part. One condition is given by

$$\Omega^2 - 2\pi G(1 + \epsilon)\Sigma_0 k + \frac{c_s^2 k^2}{1 + \epsilon} < 0. \quad (14)$$

The other case is given by

$$\Omega^2 - 2\pi G(1 + \epsilon)\Sigma_0 k + \frac{c_s^2 k^2}{1 + \epsilon} > 0, \quad (15)$$

and

$$\frac{\epsilon c_s^2 k^2}{t_{\text{stop}}} [\Omega^2 - 2\pi G(1 + \epsilon)\Sigma_0 k] + Dk^2 \left( \frac{1 + \epsilon}{t_{\text{stop}}} \right)^2 \left[ \Omega^2 - 2\pi G\Sigma_0 k + \frac{c_s^2 k^2}{1 + \epsilon} \right] < 0. \quad (16)$$

Here we use that the last term in the left hand side of the Equation(13) is always positive. From Equation (14), we obtain the condition for instability

$$Q = \frac{c_s \Omega}{\pi G \Sigma} < (1 + \epsilon)^{3/2}. \quad (17)$$

This condition is similar to the condition for the gravitational instability of the gas disk and it is completely same in the case  $\epsilon = 0$ . This instability is the gravitational instability of the gas and dust disk. In the case Equation (17) is not satisfied, the disk is unstable only if Equation (16) is satisfied. From Equation (16), the condition for instability is given by

$$\frac{c_s^2 \Omega^2 D \left[ \frac{\epsilon}{1 + \epsilon} t_{\text{stop}} c_s^2 + D(1 + \epsilon) \right]}{(\pi G \Sigma_0)^2 [\epsilon t_{\text{stop}} c_s^2 + D(1 + \epsilon)]^2} < 1. \quad (18)$$

In the case  $\epsilon \ll 1$  and  $\epsilon t_{\text{stop}} c_s^2 \ll D$ , Equation (18) is rewritten as

$$Q \lesssim (1 + \epsilon)^{1/2}. \quad (19)$$

This condition is not satisfied in the case Equation (14) is not satisfied. Therefore, the disk is stable when  $Q > (1 + \epsilon)^{3/2}$  and  $\epsilon t_{\text{stop}} c_s^2 \ll D$  is satisfied.

In the case  $\epsilon \ll 1$  and  $\epsilon t_{\text{stop}} c_s^2 \gg D$ , Equation (18) is rewritten as

$$\frac{1}{\epsilon(1 + \epsilon)t_{\text{stop}}} \frac{D\Omega^2}{(\pi G \Sigma_0)^2} \lesssim 1, \quad (20)$$

or

$$\frac{\bar{D}Q^2}{\epsilon(1 + \epsilon)t_{\text{stop}}\Omega} \lesssim 1, \quad (21)$$

where  $\bar{D} \equiv Dc_s^{-2}\Omega$  is a normalized diffusivity.

If we ignore dynamical feedback from dust grains in the gas equation of motion, the present instability reduces to the so-called secular GI (e.g., Ward 2000). In that case long-wavelength perturbations are always unstable to the secular GI, independent of the parameters  $D$ ,  $\Sigma_{\text{d0}}$ , and  $\Omega$ . However, the feedback of the friction force from dust to gas makes the long-wavelength perturbations stable, even in disks with a low dust-to-gas mass ratio. Moreover, the perturbations are stable for all wavelengths if Equation (21) is not satisfied. In this way the present instability is different from the secular GI.

## 4. DISCUSSION

### 4.1. Turbulent Viscosity, Dust Velocity Dispersion and Disk Thickness

In Sections 2 and 3, we neglected turbulent viscosity, dust velocity dispersion, and disk thickness, for simplicity. We take into account those effects in this section.

In the turbulent disk, the momentum of the gas is also diffused by the turbulent viscosity. Coefficient of kinematic viscosity is given by  $\nu = \alpha c_s^2 / \Omega$ , where  $\alpha$  is a dimensionless measure of turbulent intensity (Shakura & Sunyaev 1973). Taking into account the turbulent viscosity, we can rewrite Equations (2) as follows:

$$\begin{aligned} \Sigma \left( \frac{\partial u_i}{\partial t} + u_k \frac{\partial u_i}{\partial x_k} \right) &= -c_s^2 \frac{\partial \Sigma}{\partial x_i} - \Sigma \frac{\partial}{\partial x_i} \left( \Phi - \frac{GM_*}{r} \right) + \frac{\Sigma_d (v_i - u_i)}{t_{\text{stop}}} \\ &+ \frac{\partial}{\partial x_k} \left[ \Sigma \nu \left( \frac{\partial u_i}{\partial x_k} + \frac{\partial u_k}{\partial x_i} - \frac{2}{3} \delta_{ik} \frac{\partial u_l}{\partial x_l} \right) \right]. \end{aligned} \quad (22)$$

Then linearized equations of this equation are given as follows:

$$\begin{aligned} -i\omega \delta u_x - 2\Omega \delta u_y &= -c_s^2 \frac{ik\delta\Sigma}{\Sigma_0} - ik\delta\Phi + \frac{\epsilon(\delta v_x - \delta u_x)}{t_{\text{stop}}} \\ &- \left( \xi + \frac{4}{3}\nu \right) k^2 \delta u_x, \end{aligned} \quad (23)$$

$$-i\omega \delta u_y + \frac{\Omega}{2} \delta u_x = \frac{\epsilon(\delta v_y - \delta u_y)}{t_{\text{stop}}} - \nu k^2 \delta u_y - ik \frac{3\nu\Omega}{2\Sigma_0} \delta\Sigma. \quad (24)$$

In this case, viscous overstability also appears (Schmit & Tscharnuter 1995), but in the case  $\alpha$  is sufficiently small, the growth rate of the viscous overstability is much smaller than that of two-component secular GI. In this paper we neglect viscous overstability and focus on the two-component secular GI. The relation between turbulent viscosity and dust diffusivity is given by Youdin & Lithwick (2007) (see also Michikoshi et al. 2012);

$$\bar{D} = \frac{1 + t_{\text{stop}}\Omega + 4(t_{\text{stop}}\Omega)^2}{[1 + (t_{\text{stop}}\Omega)^2]^2} \alpha. \quad (25)$$

In a turbulent disk, velocity dispersion of the dust is estimated by Youdin & Lithwick (2007);

$$c_d^2 = \frac{1 + 2t_{\text{stop}}\Omega + (5/4)(t_{\text{stop}}\Omega)^2}{[1 + (t_{\text{stop}}\Omega)^2]^2} \alpha c_s^2. \quad (26)$$

The velocity dispersion of the dust appears in the equations of motion for the dust as pressure-like terms. Taking into account the velocity dispersion, we can rewrite Equation (4) as follows:

$$\begin{aligned} \Sigma_d \left( \frac{\partial \mathbf{v}}{\partial t} + (\mathbf{v} \cdot \nabla) \mathbf{v} \right) &= -c_d^2 \nabla \Sigma_d - \Sigma_d \nabla \left( \Phi - \frac{GM_*}{r} \right) \\ &+ \frac{\Sigma_d (\mathbf{u} - \mathbf{v})}{t_{\text{stop}}}. \end{aligned} \quad (27)$$

Then the linearized equation of this equation is given as follows:

$$-i\omega \delta v_x - 2\Omega \delta v_y = -c_d^2 \frac{ik\delta\Sigma_d}{\Sigma_0} - ik\delta\Phi + \frac{\delta u_x - \delta v_x}{t_{\text{stop}}}. \quad (28)$$

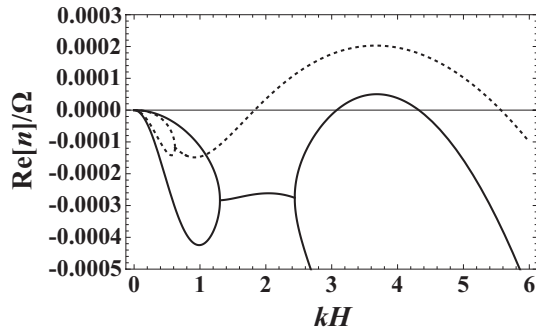


FIG. 2.— Dispersion relations of the unstable modes for  $t_{\text{stop}}\Omega = 0.01$ ,  $Q = 3$ ,  $\epsilon = 0.1$ ,  $D = 10^{-4}c_s^2\Omega^{-1}$ . Solid line shows the dispersion relation given by Equations (6), (9), (11), (23), (24), (28), and (29). Dashed line shows dispersion relation shown in Figure 1. The growth rate of the instability is decreased by the turbulent viscosity, dust velocity dispersion, and disk thickness.

Equation (12) gives the gravitational potential perturbation in the infinitesimally thin disk. However, the most unstable wavelength of the two-component secular GI is of order  $H^{-1}$  and infinitesimally thin approximation is not good approximation. The gravitational potential perturbation in the case  $k \lesssim H^{-1}$  is approximately given by Vandervoort (1970) and Shu (1984);

$$\delta\Phi = -2\pi G \left( \frac{\delta\Sigma}{1+kH} + \frac{\delta\Sigma_d}{1+kH_d} \right), \quad (29)$$

where  $H_d \sim \sqrt{\alpha/t_{\text{stop}}}\Omega H$  is the dust scale height (Cuzzi et al. 1993).

Using Equations (6), (9), (11), (23), (24), (28), and (29), we perform the linear stability analysis again. Figure 2 shows the dispersion relation given by Equations (6), (9), (11), (23), (24), (28), and (29), and the dispersion relation shown in Figure 1. The growth rate of the instability is decreased due to turbulent viscosity, dust velocity dispersion, and disk thickness.

Figure 3 shows the maximum growth rate of the unstable modes. Solid line shows the condition for instability given by Equation (21) and dashed line is given by

$$\frac{3\bar{D}Q^2}{\epsilon(1+\epsilon)t_{\text{stop}}\Omega} = 1. \quad (30)$$

The maximum  $\alpha$  for the instability is well fitted by the Equation (30). Due to the effect of the turbulent viscosity, velocity dispersion of the dust and disk thickness, the maximum  $\alpha$  for the instability is decreased by a factor of three.

#### 4.2. Dust Growth and Radial Drift

The growth rate of the instability depends on the stopping time,  $t_{\text{stop}}$ . The stopping time is given as a function of the dust radius,  $a$ , and gas density,  $\rho_g$ :

$$t_{\text{stop}} = \begin{cases} \frac{\rho_{\text{int}}a}{\rho_g c_s} & \frac{a}{l_g} < \frac{3}{2} \\ \frac{2\rho_{\text{int}}a^2}{3\rho_g c_s l_g} & \frac{a}{l_g} > \frac{3}{2} \end{cases} \quad (31)$$

where  $\rho_{\text{int}}$  is the internal density of dust and  $l_g$  is the mean free path of the gas. Therefore, the stopping time increases as the radius of dust becomes large due to coagulation.

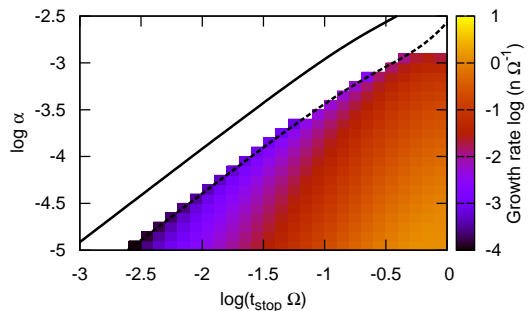


FIG. 3.— Maximum growth rate of the unstable modes for  $Q = 3$  and  $\epsilon = 0.1$ . The horizontal axis is normalized stopping time and the vertical axis is turbulence parameter,  $\alpha$ . The white region shows negative growth rate. The solid line shows the condition for instability given by Equation (21) and the dashed line is given by Equation (30).

The growth timescale of the dust is given by

$$t_{\text{grow}} = \left( \frac{d \ln m}{dt} \right)^{-1} = \frac{4}{3} \frac{\rho_{\text{int}} a}{\Delta v \rho_d}. \quad (32)$$

where  $\rho_d$  is the dust density and  $\Delta v$  is the relative velocity of the dust. In the case  $a < 3l_g/2$ , from Equations (31) and (32), the growth timescale is given by

$$t_{\text{grow}} = \frac{4}{3} \frac{\rho_g c_s t_{\text{stop}}}{\Delta v \rho_d}. \quad (33)$$

Using the relations  $\Delta v = \sqrt{t_{\text{stop}}\Omega} c_d = \sqrt{\alpha t_{\text{stop}}\Omega} c_s$  (e.g. Chiang & Youdin 2010) and  $\rho_g/\rho_d = (\Sigma/\Sigma_d)(H_d/H)$ , we obtain the growth timescale as follows (Takeuchi & Lin 2005);

$$t_{\text{grow}} = \frac{4}{3\epsilon\Omega}. \quad (34)$$

In Section 2, we adopted a uniform surface density and Keplerian rotation for both gas and dust as the background state. However, the surface density of the gas and dust depend on the radius of the disk, for example  $\Sigma \propto r^{-3/2}$  for the minimum mass Solar Nebula (Hayashi 1981). The gas is supported by pressure and rotates slightly slower than the Kepler velocity:  $\Omega_{\text{gas}} = (1-\eta)\Omega$ ,  $\eta > 0$ . Therefore, dust loses angular momentum due to gas-dust friction and drifts towards the central star. The radial drift speed is given by (Nakagawa et al. 1986)

$$v_r = -2\eta r \Omega \frac{1}{1+\epsilon} \frac{t_{\text{stop}}\Omega}{1+(t_{\text{stop}}\Omega)^2}. \quad (35)$$

In the case of the minimum mass Solar Nebula,  $\Sigma \propto r^{-3/2}$  and  $T = 280(r/1\text{AU})^{-1/2}\text{K}$ , we obtain

$$\eta = \frac{1}{2} \left( \frac{c_s}{r\Omega} \right)^2 \frac{d \ln P}{d \ln r} \simeq 1.8 \times 10^{-3} \left( \frac{r}{1\text{AU}} \right)^{\frac{1}{2}}. \quad (36)$$

Therefore, at 100 AU we obtain  $\eta \sim 10^{-2}$ . The radial

drift timescale is given by

$$t_{\text{dri}} = \frac{r}{|v_r|} = \frac{1 + \epsilon + (t_{\text{stop}}\Omega)^2}{2\eta\Omega t_{\text{stop}}\Omega}. \quad (37)$$

We assume that dusts drift inward without coagulating when  $t_{\text{grow}} \lesssim t_{\text{dri}}/30$  (Okuzumi et al. 2012). Then we obtain the critical stopping time;

$$t_{\text{stop,crit}} \simeq 0.13\Omega^{-1} \left(\frac{\epsilon}{0.1}\right) \left(\frac{\eta}{0.01}\right)^{-1} \quad (38)$$

where we assume  $\epsilon \ll 1$  and  $t_{\text{stop}}\Omega \ll 1$ . When the dust is small and  $t_{\text{stop}}$  is smaller than  $t_{\text{stop,crit}}$ , then  $t_{\text{grow}}$  is smaller than  $t_{\text{dri}}/30$ . In this case dust grows quickly and radial drift is inefficient. The stopping time becomes larger as the dust becomes larger, and dust drifts inward when  $t_{\text{grow}} = t_{\text{dri}}/30$  is satisfied. Since the gas density of the disk is larger at smaller disk radius, the stopping time of dust coming from outer disk radii is smaller than  $t_{\text{stop,crit}}$  (Equation(31)). The dust grows again to satisfy  $t_{\text{stop}} = t_{\text{stop,crit}}$  and it drifts further inwards. As a result, dust satisfying  $t_{\text{stop}} = t_{\text{stop,crit}}$  exists at each radius. Equation (30) is rewritten by using  $t_{\text{stop}} = t_{\text{stop,crit}}$ ;

$$\left(\frac{\alpha}{4 \times 10^{-5}}\right) \left(\frac{\epsilon}{0.1}\right)^{-2} \left(\frac{Q}{10}\right)^2 \left(\frac{\eta}{0.01}\right) \lesssim 1. \quad (39)$$

It is quite difficult to satisfy this condition in the MRI turbulent disk ( $\alpha \sim 0.01$ ). The maximum  $\alpha$  for the instability given by this is smaller than the  $\alpha_{\text{max}}$  given by Youdin (2011). Therefore, the effect of the back reaction from the dust to gas makes it difficult to form the planetesimal due to the secular GI even in a region without MRI.

#### 4.3. Ring Structure Formation in Protoplanetary Disks

Observations of protoplanetary disks show that ring structures form at a radius of about 100 AU. We evaluate the most unstable wavelength and the growth timescale of the instability at a radius of 100 AU for the case of a  $1M_{\odot}$  central star, a temperature of 28K, and a dust stopping time  $t_{\text{stop}} = t_{\text{stop,crit}} = 1.3 \times 10^{-1}\Omega^{-1}$ . We assume the case  $Q = 3$ , corresponding to a marginally gravitationally stable disk, a high dust-to-gas mass ratio,  $\epsilon = 0.1$ , and  $\alpha = 4 \times 10^{-4}$ . These parameters corresponding to  $\eta = 10^{-2}$ . Then, the most unstable wavelength is about 13 AU, and the growth timescale is about  $2 \times 10^4$  yr. These results are consistent with the observation because the disk lifetime is about  $10^6$  yr and the observed ring width is a few tens of AU. The dust radius that corresponds to a stopping time  $t_{\text{stop}} = 0.13\Omega^{-1}$  in this disk is about 4 mm.

The amplitude of the dust surface density eigenfunction is larger than that of gas surface density. This means that the dust-to-gas mass ratio increases as the perturbation grows. Therefore, the instability forms a ring-like structure where the dust is concentrated. If the dust is sufficiently concentrated, gravitational instability of the ring will occur and the resulting gravitational collapse and fragmentation of the ring will form planetesimals. Therefore, the present instability is important for the formation of planetesimals and rocky planet at outer disk radii of around 100AU. Planetesimals or rocky planets located at outer radii may survive disk gas dispersal.

They occasionally collide with each other over a long timescale and provide small dust if the collisions are destructive. After gas dispersal, small dust is replenished by the collisional destruction of planetesimals, and rocky planets are expected to form a debris disk of solid particles. Hence, these objects may provide a unique origin for debris disks, because the dust grains in debris disks have a short lifetime and the debris disk requires continuous replenishment of dust grains. Therefore, the two-component secular GI may play an important role in the formation of debris disks.

Some of the observed rings are not axisymmetric. To investigate non-axisymmetric accumulation of gas and dust in the azimuthal direction, we need a linear analysis for non-axisymmetric modes. Observations of the dust continuum show the dust surface density is about 10 times larger than that of the gap. To compare the resultant structure of the instability with observations, we have to investigate the non-linear effects of the instability. In this work we treat the dust as a fluid that diffuses out by the gas turbulence with diffusivity  $D$ . Since the condition for the instability depends on  $D$ , a more realistic treatment of the dust is important for further analysis.

If ring structures formed by the two-component secular GI are observed, it may be an indicator of the dust concentration and weak turbulence in the disk.

#### 4.4. Comparison with the Previous Works

The secular GI has been investigated for planetesimal formation. Ward (1976, 2000) has performed the linear stability analysis of the secular GI taking into account the velocity dispersion of the dust particles (see Section 4.1), but not taking into account the diffusion due to the turbulence. Youdin (2011) takes into account the diffusion due to the turbulence and found that the dust diffusion decreases the growth rate of the secular GI. These previous works solved only the equations for dust in the Keplerian rotation gas disk. They did not take into account the back reaction from the dust to the gas since the surface density of the dust is usually much smaller than that of gas. In this work, we take into account the back reaction and solve equations for both gas and dust. We have found that when the growth timescale of the instability is much longer than the dynamical timescale, the back reaction is not negligible even if the surface density of the dust is smaller than that of gas. In such a case, Coriolis force stabilizes the long wavelength perturbations. The condition for the two-component secular GI is approximately given by Equation (16). Therefore, the terms proportional to  $\Omega^2$  stabilize the long wavelength perturbations. In the following, we show that these terms come from the Coriolis force. From the equations of motion for gas and dust, the equations for the relative velocity are given by

$$-2\Omega(\delta v_y - \delta u_y) = c_s^2 \frac{ik\delta\Sigma}{\Sigma_0} + \frac{1+\epsilon}{t_{\text{stop}}}(\delta u_x - \delta v_x), \quad (40)$$

$$\frac{\Omega}{2}(\delta v_x - \delta u_x) = \frac{1+\epsilon}{t_{\text{stop}}}(\delta u_y - \delta v_y), \quad (41)$$

where we use  $|\omega| \ll t_{\text{stop}}^{-1}$  (terminal velocity approximation). Using (6) and (41) to eliminate  $\delta\Sigma$ ,  $\delta u_y$  and  $\delta v_y$

from (40), we obtain

$$\begin{aligned} & \left[ \Omega^2 + \left( \frac{1+\epsilon}{t_{\text{stop}}} \right)^2 \right] \delta v_x \\ &= \left[ \Omega^2 + i \frac{c_s^2 k^2}{\omega} \frac{1+\epsilon}{t_{\text{stop}}} + \left( \frac{1+\epsilon}{t_{\text{stop}}} \right)^2 \right] \delta u_x. \end{aligned} \quad (42)$$

In the case that the dust is small and hence,  $\Omega \ll t_{\text{stop}}^{-1}$ , Equation (42) is rewritten as

$$\delta v_x = \left( \frac{c_s^2 k^2}{n} \frac{t_{\text{stop}}}{1+\epsilon} + 1 \right) \delta u_x. \quad (43)$$

Hereafter, we assume that pressure term  $c_s^2 k^2$  is large and  $c_s^2 k^2 t_{\text{stop}} / (n(1+\epsilon)) \gg 1$  is satisfied. This condition is satisfied for example in the case  $Q = 3$  and  $kH \sim 2$ . Using this approximation, we obtain

$$\delta v_x = \frac{c_s^2 k^2}{n} \frac{t_{\text{stop}}}{1+\epsilon} \delta u_x \gg \delta u_x. \quad (44)$$

This means that the radial motion of the gas is suppressed by the pressure and it is negligible compared to the radial motion of the dust. Therefore, the relative velocity in the y-direction is given by

$$\delta u_y - \delta v_y \simeq \frac{\Omega t_{\text{stop}}}{2(1+\epsilon)} \delta v_x \ll \delta v_x \quad (45)$$

From Equations (8) and (11), we also obtain the equation of the centroid velocity in the y-direction

$$n(\delta u_y + \epsilon \delta v_y) + \frac{\Omega}{2}(\delta u_x + \epsilon \delta v_x) = 0. \quad (46)$$

Using (44) and (45), we can rewrite Equation (46) as

$$n(1+\epsilon)\delta v_y + \frac{\epsilon\Omega}{2}\delta v_x = 0. \quad (47)$$

Thus, we can rewrite Equation (10) as follows,

$$\frac{\epsilon}{1+\epsilon} \frac{\Omega^2}{n} \delta v_x = 2\pi G \frac{k\epsilon\Sigma_0}{n + Dk^2} \delta v_x - \frac{\delta v_x}{t_{\text{stop}}}. \quad (48)$$

(We can derive the same equation from the equation for the centroid velocity in the x-direction instead of Equation (10).) Thus, we obtain the dispersion relation,

$$\begin{aligned} & n^2 + \left\{ \frac{\epsilon t_{\text{stop}}}{1+\epsilon} [\Omega^2 - 2\pi G(1+\epsilon\Sigma_0 k)] + Dk^2 \right\} n \\ &+ \frac{\epsilon t_{\text{stop}}}{1+\epsilon} \Omega^2 Dk^2 = 0. \end{aligned} \quad (49)$$

This is approximately same as Equation (13) in the case  $c_s^2 k^2 \gg \Omega^2 - 2\pi G\Sigma_0 k$ . The condition for the instability is given by

$$\left\{ \frac{\epsilon t_{\text{stop}}}{1+\epsilon} [\Omega^2 - 2\pi G(1+\epsilon\Sigma_0 k)] + Dk^2 \right\} n < 0. \quad (50)$$

Therefore, the long wavelength perturbations are stabilized by the term proportional to  $\Omega^2$ . This term comes from the Coriolis force acting on the dust. Thus we conclude that Coriolis force stabilizes the long wavelength

perturbations. The relations of the velocities of the gas and the dust  $\delta v_x \gg \delta u_x$  and  $\delta v_y \sim \delta u_y$  are essential in understanding the effect of the back reaction. As mentioned above, the radial motion of the gas is suppressed by the pressure (Equation (40)). On the other hand, there is no force to suppress the rotational velocity of the gas. Therefore, the rotational velocity of the gas is similar to that of the dust (Equation (45)). The Coriolis force due to the radial velocity of the dust accelerates the dust in the y-direction and also gas through friction. Although the left hand side of Equation (48) is suppressed by a factor  $\epsilon/(1+\epsilon)$ , this term remains and stabilize the long wavelength perturbations.

If the back reaction is neglected, the equation of motion of the dust in the y-direction is approximately given by

$$\frac{\Omega}{2} \delta v_x = -\frac{\delta v_y}{t_{\text{stop}}}, \quad (51)$$

where we use the terminal velocity approximation ( $|n| \ll t_{\text{stop}}^{-1}$ ). This equation means that the Coriolis force balances the frictional drag force. In this case, the long-wavelength perturbations appear to be always unstable. Thus, in Youdin (2011) the maximum  $\alpha$  for the secular GI is given by the condition  $n^{-1} = t_{\text{dri}}$ . However,  $t_{\text{dri}}$  is usually much larger than the dynamical timescale. Therefore the back reaction should not be neglected and it lowers the maximum  $\alpha$  for the instability. Coradini et al. (1981) also solve the equations for both the gas and the dust but they focused on dust rich disks. In general, the existence of the growth rate much smaller than the dynamical timescale corresponds to the near cancellation of various acceleration terms in equation of motion for the unstable mode. In this case, even a very small term possibly contributes significantly to the growth rate, and thus, should not be neglected.

## 5. SUMMARY

We investigate instability due to gas-dust friction in protoplanetary disks by a local analysis using two-fluid equations for gas and dust. This instability is reduced to the secular GI if we ignore dynamical feedback from dust grains in the gas equation of motion. We obtain the approximate dispersion relation, Equation (13), and the condition for the instability, Equation (30). We found that the long-wavelength perturbations are stabilized due to the feedback. The condition for the instability of the full treatment of gas and dust is more difficult to be satisfied than the condition for the secular GI derived by Youdin (2011) because of the back reaction of the frictional force from dust to gas. In the case  $Q \sim 3$ , corresponding to a marginally gravitationally stable disk, a high dust-to-gas mass ratio,  $\epsilon \gtrsim 0.1$ , and weak turbulence  $\alpha \lesssim 4 \times 10^{-4}$  are required for the instability and the growth timescale is about  $2 \times 10^4$  yr if  $\epsilon \sim 0.1$ . Since the instability grows when dust to gas ratio is enhanced and turbulence is weak, the observation of ring-like structures may be an indicator of a dust-concentrated, weekly turbulent disk.

We thank Takashi Nakamura for his continuous encouragement and Hiroshi Kobayashi, Satoshi Okuzumi and Kohei Inayoshi for fruitful discussion. We also thank Jennifer M. Stone for useful comments. This work was supported by Grant-in-Aid for JSPS Fellows.

## REFERENCES

- Andrews, S. M., Wilner, D. J., Espaillat, C., et al. 2011, *ApJ*, 732, 42
- Casassus, S., van der Plas, G., M., S. P., et al. 2013, *Nature*, 493, 191
- Chiang, E., & Youdin, A. N. 2010, *Annual Review of Earth and Planetary Sciences*, 38, 493
- Coradini, A., Magni, G., & Federico, C. 1981, *A&A*, 98, 173
- Cuzzi, J. N., Dobrovolskis, A. R., & Champney, J. M. 1993, *Icarus*, 106, 102
- Fukagawa, M., Tamura, M., Itoh, Y., et al. 2006, *ApJ*, 636, L153
- Fukagawa, M., Tsukagoshi, T., Momose, M., et al. 2013, *ArXiv e-prints*, arXiv:1309.7400
- Geers, V. C., Pontoppidan, K. M., van Dishoeck, E. F., et al. 2007, *A&A*, 469, L35
- Goldreich, P., & Lynden-Bell, D. 1965, *MNRAS*, 130, 125
- Hashimoto, J., Tamura, M., Muto, T., et al. 2011, *ApJ*, 729, L17
- Hashimoto, J., Dong, R., Kudo, T., et al. 2012, *ApJ*, 758, L19
- Hayashi, C. 1981, in *IAU Symposium, Vol. 93, Fundamental Problems in the Theory of Stellar Evolution*, ed. D. Sugimoto, D. Q. Lamb, & D. N. Schramm, 113–126
- Hayashi, C., Nakazawa, K., & Nakagawa, Y. 1985, in *Protostars and planets II (A86-12626 03-90)*, Tucson, AZ, University of Arizona Press, 1985, p. 1100-1153., ed. D. C. Black & M. S. Matthews, 1100–1153
- Isella, A., Natta, A., Wilner, D., Carpenter, J. M., & Testi, L. 2010, *ApJ*, 725, 1735
- Isella, A., Pérez, L. M., & Carpenter, J. M. 2012, *ApJ*, 747, 136
- Isella, A., Pérez, L. M., Carpenter, J. M., et al. 2013, *ApJ*, 775, 30
- Johansen, A., & Youdin, A. 2007, *ApJ*, 662, 627
- Kley, W., & Nelson, R. P. 2012, *ARA&A*, 50, 211
- Lin, D. N. C., & Papaloizou, J. 1986, *ApJ*, 309, 846
- Lin, D. N. C., & Papaloizou, J. C. B. 1993, in *Protostars and Planets III*, ed. E. H. Levy & J. I. Lunine, 749–835
- Lyra, W., & Kuchner, M. 2013, *Nature*, 499, 184
- Lyra, W., & Kuchner, M. J. 2012, *ArXiv e-prints*, arXiv:1204.6322
- Mathews, G. S., Williams, J. P., & Ménard, F. 2012, *ApJ*, 753, 59
- Mayama, S., Hashimoto, J., Muto, T., et al. 2012, *ApJ*, 760, L26
- Michikoshi, S., Kokubo, E., & Inutsuka, S.-i. 2012, *ApJ*, 746, 35
- Nakagawa, Y., Sekiya, M., & Hayashi, C. 1986, *Icarus*, 67, 375
- Narayan, R., Goldreich, P., & Goodman, J. 1987, *MNRAS*, 228, 1
- Okuzumi, S., Tanaka, H., Kobayashi, H., & Wada, K. 2012, *ApJ*, 752, 106
- Schmit, U., & Tscharnuter, W. M. 1995, *Icarus*, 115, 304
- Shakura, N. I., & Sunyaev, R. A. 1973, *A&A*, 24, 337
- Shu, F. H. 1984, in *IAU Colloq. 75: Planetary Rings*, ed. R. Greenberg & A. Brahic, 513–561
- Takeuchi, T., & Lin, D. N. C. 2005, *ApJ*, 623, 482
- Takeuchi, T., Miyama, S. M., & Lin, D. N. C. 1996, *ApJ*, 460, 832
- van der Marel, N., van Dishoeck, E. F., Bruderer, S., et al. 2013, *Science*, 340, 1199
- Vandervoort, P. O. 1970, *ApJ*, 161, 87
- Ward, W. R. 1976, in *Frontiers of Astrophysics*, ed. E. H. Avrett, 1–40
- Ward, W. R. 2000, *On Planetesimal Formation: The Role of Collective Particle Behavior*, ed. R. M. Canup, K. Righter, & et al., 75–84
- Youdin, A., & Johansen, A. 2007, *ApJ*, 662, 613
- Youdin, A. N. 2011, *ApJ*, 731, 99
- Youdin, A. N., & Goodman, J. 2005, *ApJ*, 620, 459
- Youdin, A. N., & Lithwick, Y. 2007, *Icarus*, 192, 588
- Zhu, Z., Nelson, R. P., Hartmann, L., Espaillat, C., & Calvet, N. 2011, *ApJ*, 729, 47